

NEW TRIANGULAR MASS-LUMPED FINITE ELEMENTS OF DEGREE SIX FOR WAVE PROPAGATION

William A. Mulder^{1, 2, *}

¹Shell Global Solutions International, P. O. Box 60, 2280 AB Rijswijk, The Netherlands

²Faculty of Civil Engineering and Geotechnology, Delft University of Technology, P. O. Box 5048, 2600 GA Delft, The Netherlands

Abstract—Mass-lumped continuous finite elements allow for explicit time stepping with the second-order wave equation if the resulting integration weights are positive and provide sufficient accuracy. To meet these requirements on triangular and tetrahedral meshes, the construction of continuous finite elements for a given polynomial degree on the edges involves polynomials of higher degree in the interior. The parameters describing the supporting nodes of the Lagrange interpolating polynomials and the integration weights are the unknowns of a polynomial system of equations, which is linear in the integration weights. To find candidate sets for the nodes, it is usually required that the number of equations equals the number of unknowns, although this may be neither necessary nor sufficient. Here, this condition is relaxed by requiring that the number of equations does not exceed the number of unknowns. This resulted in two new types elements of degree 6 for symmetrically placed nodes. Unfortunately, the first type is not unisolvent. There are many different elements of the second type with a large range in their associated time-stepping stability limit. To assess the efficiency of the elements of various degrees, numerical tests on a simple problem with an exact solution were performed. Efficiency was measured by the computational time required to obtain a solution at a given accuracy. For the chosen example, elements of degree 4 with fourth-order time stepping appear to be the most efficient.

Received 13 May 2013, Accepted 31 July 2013, Scheduled 5 August 2013

* Corresponding author: William Alexander Mulder (Wim.Mulder@shell.com).

1. INTRODUCTION

The finite-difference method is an attractive tool for the numerical solution of the wave equation. It is easy to code up and straightforward to parallelize. Its accuracy degrades, however, in the presence of sharp contrasts in material properties. Finite elements provide superior accuracy if the mesh follows the interfaces between different materials.

Finite-element discretization of the second-order wave equation leads to a stiffness and a mass matrix. Mass lumping avoids the cost of inverting the latter and allows for explicit time stepping. To maintain the spatial accuracy and time-stepping stability, the weights obtained by mass lumping should be positive and provide sufficient accuracy [1].

We would like to have finite elements that are (i) conforming, (ii) have a symmetric placement of nodes, (iii) are unisolvent, (iv) no loss of accuracy compared to elements without lumping, and (v) lead to positive weights after lumping. The standard polynomial finite elements on triangles or tetrahedra can meet these requirements only for the one of lowest degree, the linear element. Elements of higher degree on triangles require enrichment with polynomials of still higher degree that reduce to the desired degree at the edges [1–3]. In 3D, the degrees on the edges and faces and interior may all be different [4]. So far, there exist triangular elements of degree 2 [1], 3 [2, 3], 4 [4], and 5 [5] on the edges, as well as tetrahedral elements of degree 2 [4] and 3 [5]. The triangular elements of degree 6 and 7, constructed by [6], have their accuracy too low by one order for the second-order wave equation.

Mass lumping is related to numerical quadrature. Given a reference element, the row sums of its contribution to the mass matrix are identical to numerical integration weights with a certain accuracy. As there is a map from the triangle to one octant of the surface of a sphere, there is a relation between quadrature on either [7–9]. The requirement of continuity across element boundaries provides an additional constraint.

To construct an integration rule that is accurate for polynomials up to a certain degree, a set of integration nodes need to be found, together with integration weights. Numerical integration of all the polynomials up to the given degree should provide the same as exact integration. Consistency conditions [5, 8, 10, 11] limit the choice of integration nodes to cases where the number of unknowns, involving the parametrization of the nodes and the integration weights, equals the number of equations. This leads to so-called rule patterns. Here, this requirement will be relaxed by allowing the number of unknowns

to exceed the number of equations.

Section 2 provides a review of the approach to the construction of elements, following [5]. A new aspect is the parametrization of the nodes, which simplifies the symbolic computations. Section 3 presents two types of new elements of degree 6 of which only one type is useful. Since it is not unique, several elements of this type are listed. Section 4 describes numerical tests, carried out to assess the relative performance for elements of degrees 1 to 6. A discussion and conclusion follows at the end.

2. METHOD

2.1. Requirements

The motivation for this work is the second-order wave equation

$$\frac{1}{c^2} \frac{\partial^2 u}{\partial t^2} - \Delta u = s,$$

with $c(\mathbf{x})$ the velocity as a function of position \mathbf{x} , $u(t, \mathbf{x})$ the solution as a function of time t and position, and $s(t, \mathbf{x})$ an optional source term. The latter can have the form $s(t, \mathbf{x}) = w(t)\delta(\mathbf{x} - \mathbf{x}_s)$, with $w(t)$ the signature or wavelet of a point source located at \mathbf{x}_s . Initial values are $u(0, \mathbf{x})$ and $\partial u / \partial t(0, \mathbf{x})$. These are usually set to zero in the presence of a source term. Dirichlet, Neumann, or radiation boundary conditions are supplied on the boundary of the domain $\Omega \subset \mathbb{R}^n$ ($n = 2$ in this paper). Its finite-element discretization with Lagrange polynomials as basis functions leads to a mass and stiffness matrix. To enable explicit time-stepping, the mass matrix is replaced by its diagonal, lumped version by taking row sums per element.

As already mentioned in the introduction, the following requirements are imposed in this paper: (i) conformity or continuity of the solution across element boundaries, (ii) symmetric arrangement of nodes, (iii) unisolvency, (iv) no loss of accuracy due to lumping, (v) positive integration weights. The last condition is necessary for numerical stability if a standard second-order time-stepping scheme is used for the explicit time stepping. Among the elements that obey these conditions, those with the smallest number of nodes are usually preferred for efficiency.

Conformity for polynomials of highest degree M requires $M + 1$ points on the edges, including the vertices, leading to $3M$ points on the boundary of each triangular element. To support Lagrange polynomials of degree M on the triangle, given by the set P_M , a total of $\frac{1}{2}(M + 1)(M + 2)$ nodes are required, leaving $\frac{1}{2}(M - 2)(M - 1)$ points for the interior. As it turns out, elements with these nodes

cannot provide positive integration weights except for the standard linear element of degree $M = 1$.

To obtain positive integration weights, polynomials of degree M' , usually larger than M , can be chosen in the interior of the triangle. These should vanish on the element boundaries. If we consider the reference element with points (x, y) , $0 \leq x \leq 1$, $0 \leq y \leq 1$, $0 \leq 1 - x - y \leq 1$, the space of the additional polynomials can be characterized by $P_{M'-3} \times [b]$, with bubble function $b = xy(1 - x - y)$ and $[b]$ the subspace generated by this function. The space of Lagrange polynomials is then $P_M \oplus P_{M'-3} \times [b]$. The total number of nodes becomes $3M + \frac{1}{2}(M' - 2)(M' - 1)$ as compared to $\frac{1}{2}(M + 1)(M + 2)$ for the standard elements.

The numerical integration rule should be accurate up to degree $q = M + M' - 2$ [12]. The -2 term is due to the second-order spatial derivatives in the wave equation.

2.2. Rule Patterns

The requirement that the node be symmetrically arranged means that nodes should be selected from one of the 6 equivalence classes listed in Table 1. The classes are enumerated sequentially, with classes 1–3 referring to the boundary and 4–6 to the interior. This differs from the notation in [5, 8, 10].

Table 1. Equivalence classes for the triangle. For each class, one of the nodes is specified on the reference element. The number of nodes per class is n_c .

class	node	n_c	type
1	(0, 0)	3	vertices
2	(1/2, 0)	3×1	edge midpoints
3	(α , 0)	3×2	interior edge points
4	(1/3, 1/3)	1	center
5	(α , α)	3	interior
6	(α , β)	6	interior

A rule pattern K is a set of 6 numbers, defining the number of nodes selected from each class. The standard linear element has $K = \{1, 0, 0, 0, 0, 0\}$. The pattern should be able to support the Lagrange polynomials used as basis functions for the finite-element discretization.

Given a rule pattern, the requirement that numerical quadrature be exact up to a certain degree q yields a system of equations that is

polynomial in the parameters describing the nodes and linear in the integration weights. Following [5, 8, 10, 11], the choice of polynomials can be restricted to those of the form $f_{l,m} = (xy)^l(1 - x - y)^m$ with $0 \leq 2l + m \leq q$ and $0 \leq m \leq l$. The system of equations becomes

$$\int_0^1 dx \int_0^{1-x} dy f_{l,m} = \sum_{i=1}^6 \sum_{j=1}^{K_i} w_{i,j} \sum_{k=1}^{n_{ci}} f_{l,m}(x_{i,j,k}, y_{i,j,k}), \tag{1}$$

$$0 \leq 2l + m \leq q, \quad 0 \leq m \leq l.$$

The summations are carried out over class i , the corresponding set of nodes j , if any, and the total of n_{ci} nodes that can be obtained from one point by the symmetries of the triangle, the dihedral group of order 6. If that one point is $(x_{i,j,1}, y_{i,j,1})$ for a given class i and point j , the other nodes $(x_{i,j,k}, y_{i,j,k})$, $k = 2, \dots, n_{ci}$, can simply be obtained by taking the first pair of each of the permutations of the triple $(x_{i,j,1}, y_{i,j,1}, 1 - x_{i,j,1} - y_{i,j,1})$. The unknowns are the integration weights $w_{i,j}$ and the parameters that define the nodes for classes 3, 5, and 6, as listed in the second column of Table 1.

2.3. Selection of Nodes

Because the system (1) may be difficult to solve, it is natural to restrict the number of choices by ensuring that the number of equations equals the number of unknowns [5, 8, 10, 11]. Here, this condition is relaxed by requiring that the number of equations n_e does not exceed the number of unknowns n_u . The condition $n_u \geq n_e$ is necessary nor sufficient, but it is unlikely that a solution will exist otherwise.

Table 2 contains earlier results of Table 5 in [5] and extends it beyond degree $M = 5$. The first pair of columns define the degrees of the polynomials on the edges, M , and in the interior, M' . The third lists the degree q for which quadrature should be exact. We should have $q = M + M' - 2$, but there are two exceptions, considered by [6] and marked here by an asterisk. For given $\{M, M', q\}$, there may be several rule patterns K , in which case an additional version number, v , is included. A node set for quadrature is labeled by $\{M, M', q, v\}$. The fifth column of Table 2 lists the main result, the rule pattern K defining the number of nodes selected from each class. The following 3 columns define the number of equations, n_e , of the polynomial system, the number of unknowns, n_u , which are the node parameters and integration weights, and the total number of nodes $n = \sum_{i=1}^6 K_i n_{ci}$. The last column contains remarks related to the results found in Section 3 and includes references for known elements. In the absence of a remark, it is presently unknown whether or not a proper solution exists.

2.4. Parametrization

A suitable parametrization, different from the one in column 2 of Table 1, can result in a simpler form of the system of polynomial equations. Consider, for instance, the node $(\alpha, 0)$ of class 3, a point on the edge with $0 < \alpha < \frac{1}{2}$ excluding the vertex (class 1, $\alpha = 0$) and midpoint (class 2, $\alpha = \frac{1}{2}$). Given one point in an equivalence class, the set of nodes can be found by taking all the permutations of $(x, y, 1 - x - y)$ and dropping the last entry of each triple. For $(\alpha, 0)$,

Table 2. Rule patterns. M is the degree on the edges, M' in the interior, quadrature is exact through degree q . Versions are labeled by v , K defines the number of points for each equivalence class, not counting their symmetric counterparts, with K_j corresponding to class j . The number of equations is n_e , the number of unknowns (weights and position parameters) is n_u , and the total number of nodes is n .

M	M'	q	v	K	n_e	n_u	n	remarks
1	1	1		1, 0, 0, 0, 0, 0	1	1	3	OK
2	2	2		1, 1, 0, 0, 0, 0	2	2	6	zero weight
	3	3		1, 1, 0, 1, 0, 0	3	3	7	OK, [1]
	4	4		1, 1, 0, 0, 1, 0	4	4	9	OK
3	3	4		1, 0, 1, 1, 0, 0	4	4	10	neg. weight
	4	5		1, 0, 1, 0, 1, 0	5	5	12	OK, [2, 3]
	5	6		1, 0, 1, 0, 2, 0	7	7	15	OK
4	5	7		1, 1, 1, 0, 2, 0	8	8	18	OK, [4]
	6	8		1, 1, 1, 1, 1, 1	10	10	22	OK
5	6	9		1, 0, 2, 1, 3, 0	12	12	25	no solution
	7	10	1	1, 0, 2, 0, 3, 1	14	14	30	OK, [5]
			2	1, 0, 2, 0, 5, 0	14	15	30	no solution
6	7	11		1, 1, 2, 0, 5, 0	16	16	33	no solution
	8	12	1	1, 1, 2, 0, 5, 1	19	19	39	complex α on edge
			2	1, 1, 2, 0, 7, 0	19	20	39	no solution
	9	12*		1, 1, 2, 1, 3, 3	19	22	46	[6], q too small
	9	13	1	1, 1, 2, 1, 1, 4	21	21	46	not unisolvent
			2	1, 1, 2, 1, 3, 3	21	22	46	OK
			3	1, 1, 2, 1, 5, 2	21	23	46	
			4	1, 1, 2, 1, 7, 1	21	24	46	
			5	1, 1, 2, 1, 9, 0	21	25	46	no solution

7	8	13		1, 0, 3, 0, 7, 0	21	21	42	no solution
	9	14	1	1, 0, 3, 1, 5, 2	24	24	49	
			2	1, 0, 3, 1, 7, 1	24	25	49	no solution
			3	1, 0, 3, 1, 9, 0	24	26	49	no solution
	10	14*		1, 0, 3, 0, 4, 3	24	24	51	[6], q too small
	10	15	1	1, 0, 3, 0, 4, 4	27	27	57	
			2	1, 0, 3, 0, 6, 3	27	28	57	
			3	1, 0, 3, 0, 8, 2	27	29	57	
			4	1, 0, 3, 0, 10, 1	27	30	57	no solution
			5	1, 0, 3, 0, 12, 0	27	31	57	no solution
	11	16	1	1, 0, 3, 0, 1, 7	30	30	66	
			2	1, 0, 3, 0, 3, 6	30	31	66	
			3	1, 0, 3, 0, 5, 5	30	32	66	
			4	1, 0, 3, 0, 7, 4	30	33	66	
			5	1, 0, 3, 0, 9, 3	30	34	66	
			6	1, 0, 3, 0, 11, 2	30	35	66	
			7	1, 0, 3, 0, 13, 1	30	36	66	no solution
			8	1, 0, 3, 0, 15, 0	30	37	66	no solution
8	9	15		1, 1, 3, 1, 9, 0	27	27	52	no solution
	10	16	1	1, 1, 3, 0, 8, 2	30	30	60	
			2	1, 1, 3, 0, 10, 1	30	31	60	
			3	1, 1, 3, 0, 12, 0	30	32	60	
	11	17	1	1, 1, 3, 0, 5, 5	33	33	69	
			2	1, 1, 3, 0, 7, 4	33	34	69	
			3	1, 1, 3, 0, 9, 3	33	35	69	
			4	1, 1, 3, 0, 11, 2	33	36	69	
			5	1, 1, 3, 0, 13, 1	33	37	69	no solution
			6	1, 1, 3, 0, 15, 0	33	38	69	no solution
	12	18	1	1, 1, 3, 1, 2, 8	37	37	79	
			2	1, 1, 3, 1, 4, 7	37	38	79	
			3	1, 1, 3, 1, 6, 6	37	39	79	
			4	1, 1, 3, 1, 8, 5	37	40	79	
			5	1, 1, 3, 1, 10, 4	37	41	79	
			6	1, 1, 3, 1, 12, 3	37	42	79	
			7	1, 1, 3, 1, 14, 2	37	43	79	
			8	1, 1, 3, 1, 16, 1	37	44	79	
			9	1, 1, 3, 1, 18, 0	37	45	79	no solution

this results in

$$\{(\alpha, 0), (0, \alpha), (\alpha, 1 - \alpha), (1 - \alpha, \alpha), (1 - \alpha, 0), (0, 1 - \alpha)\}. \quad (2)$$

As already mentioned, we only need to consider polynomials of the form $f_{l,m}(x, y) = (xy)^l(1 - x - y)^m$ with $0 \leq m \leq l$. Its numerical integration in Equation (1) produces a polynomial

$$C_{i,l,m} = \sum_{k=1}^{n_{c_i}} f_{l,m}(x_{i,j,k}, y_{i,j,k}),$$

where i enumerates the class, j refers to one of the K_i nodes for that class, and $(x_{i,j,k}, y_{i,j,k})$, $k = 1, \dots, n_{c_i}$ refers to the full set of nodes that can be obtained by symmetry. For class 3, $C_{3,l,m}$ is zero with the exception of

$$C_{3,0,0} = n_{c_3} = 6, \quad C_{3,l,0} = 2[\alpha(1 - \alpha)]^l, \quad l > 0.$$

The dependence on α with $0 < \alpha < 1$ suggests the choice $\alpha = \frac{1}{2}(1 - \sqrt{1 - \tilde{\alpha}})$ with $0 < \tilde{\alpha} < 1$, leading to $C_{3,l,0} = 2(\tilde{\alpha}/4)^l$ for $l > 0$.

For class 5 with point (α, α) , $0 < \alpha < \frac{1}{2}$,

$$C_{5,m+k,m} = \alpha^{2m+k}(1 - 2\alpha)^m [2(1 - 2\alpha)^k + \alpha^k],$$

where $k = m - l \geq 0$. It is not clear to me how to simplify this with a suitable substitution for α .

Class 6 has (α, β) with, for instance, $0 < \alpha < \frac{1}{2}$, $0 < \beta < \min(\alpha, 1 - 2\alpha)$. Then,

$$C_{6,m+k,m} = 2[\alpha\beta(1 - \alpha - \beta)]^m \left\{ [\alpha\beta]^k + [\alpha(1 - \alpha - \beta)]^k + [\beta(1 - \alpha - \beta)]^k \right\}.$$

One choice that simplifies this expression is $\beta = \frac{1}{2}(1 - \alpha)(1 - w)$, yielding

$$C_{6,m+k,m} = \frac{2}{4^{m+k}} [\alpha(1 - \alpha)^2(1 - w^2)]^m \left\{ (1 - w^2)^k (1 - \alpha)^{2k} + [2\alpha(1 - \alpha)]^k F_k(w) \right\}.$$

Here, $F_k(w) = (1 - w)^k + (1 + w)^k$. Its expansion produces a sum with only even powers of w . Therefore, $C_{6,m+k,m}$ depends on w^2 . This suggests the substitution $\beta = \frac{1}{2}(1 - \alpha)(1 - \sqrt{1 - \tilde{\beta}})$, $0 < \tilde{\beta} \leq 1$.

Another choice is $u = 3[(\alpha + \beta) - (\alpha^2 + \alpha\beta + \beta^2)]$, $v = 27\alpha\beta(1 - \alpha - \beta)$. Its inverse has 6 solutions for (α, β) , one of which suffices to characterize the 6 nodes in the equivalence class. Then,

$$C_{6,m+k,m} = 6 \left(\frac{v}{27}\right)^m \frac{g_k(u, v)}{9^k},$$

with $g_k(u, v)$ a polynomial in u and v . The ones of lowest degree are $g_0(u, v) = 1$, $g_1(u, v) = u$, $g_2(u, v) = 3u^2 - 2v$, $g_3(u, v) = 9u(u^2 - v) + v^2$, $g_4(u, v) = 9u^2(3u^2 - 4v) + 2(2u + 3)v^2$. The domain of u and v that defines proper points is a subset of $u \in (0, 1)$, $v \in (0, 1)$, given by $\max(0, 1 - 3\tilde{u} - 2\tilde{u}^{3/2}) < v < 1 - 3\tilde{u} + 2\tilde{u}^{3/2}$, with $\tilde{u} = 1 - u$. Note that the lower bound of v is positive if $3/4 < u < 1$.

2.5. Polynomial System

The polynomial system can be expressed as $A\mathbf{w} = \mathbf{b}$, with the vector \mathbf{w} containing the $n_w = \sum_{i=1}^6 K_i$ integration weight and \mathbf{b} the results of exact integration. Both the matrix A , with n_e rows and n_w columns, and the vector \mathbf{b} consist of polynomials in the node parameters.

For the elements of lower degree, a symbolic algebra package will readily provide a solution. For elements of higher degree, a Gröbner basis approach may still provide a negative result after running for a fairly short time in cases where a solution does not exist. However, given its exponential complexity, it usually runs out of computer memory after hours or days if there are one or more solutions.

As an alternative, a symbolic procedure was coded that attempts to reduce the matrix A to upper block triangular form, using polynomial quotients but avoiding rational functions and fractions. In that way, a possibly simpler polynomial system can be obtained. The result depends on the ordering of the nodes and the unknowns. We can, for instance, adopt the ordering implicit in Table 1, so classes 1 to 6, or take classes 1, 2, 4, 3, 5, 6 with parameter-free nodes first. This procedure had already been used to find the elements reported in [13]. For the current paper, it readily identified the non-existence of solutions, which then could be confirmed independently by a Gröbner basis approach. However, for elements of degree above 4, it did not produce positive results.

Newton's method is the obvious choice to compute a numerical solution of the polynomial system. The use of the pseudo-inverse of the Jacobian of the system of equations helps in the presence of a null space. Given the oscillatory character of polynomials, the behavior of the method will strongly depend on the initial choice of parameters. Once a root has been found, a computation of the null space of the Jacobian at that root, if any, gives an indication about where nearby roots may be found.

In some cases, with $n_u = n_e$, the solution did not exist anyway. In other cases, with $n_u > n_e$ but also for $n_u = n_e$, multiple solutions may exist. Once a solution is found, it should be verified that the weights are positive and nodes lie within the element. Among several elements

for a given degree M , the one with the lowest computational cost is to be preferred. In case of multiple roots or different rule patterns with the same number of nodes, one could consider other criteria for node selection, for instance, the spatial accuracy or the Courant-Friedrichs-Lewy (CFL) condition [14] that determines the maximum allowable time step of an explicit time-stepping scheme. An example can be found in 3D for degree 3: there are two solutions for the same rule pattern with comparable spatial accuracy and one allows for a larger maximum time step than the other [15].

3. RESULTS

The last column of Table 2 indicates if a solution has been found and if it is proper. An empty line corresponds to an as yet unknown status. In all cases where the triangular simplification procedure indicated the non-existence of a solution, this could be confirmed by a Gröbner basis approach.

Table 3 lists the integration weights in column 5 and node parameters in their simplest form in column 6. For class 3, only α is given, corresponding to the point $(\alpha, 0)$ on the reference triangle as well as the points that follow by symmetry, as specified in Equation (2). Class 5 has a parameter α and 3 nodes

$$\{(\alpha, \alpha), (\alpha, 1 - 2\alpha), (1 - 2\alpha, \alpha)\}. \quad (3)$$

For class 6, the two parameters α and β correspond to the 6 points

$$\begin{aligned} \{(\alpha, \beta), (\beta, \alpha), (\alpha, 1 - \alpha - \beta), (1 - \alpha - \beta, \alpha), \\ (\beta, 1 - \alpha - \beta), (1 - \alpha - \beta, \beta)\} \end{aligned} \quad (4)$$

on the reference triangle.

For $\{5, 7, 10, 1\}$, there happens to be the relation $w_{6,1} = 27/[61600v\{u^2(3 - 4u) - v(4 - 6u + v)\}]$. The full solution has only been found in numerical form [5].

The element $\{6, 8, 12, 1\}$ has a solution. Partial elimination provides $u = 9/13$ and $v = 27/91$ for the node set of class 6 in the interior and $\tilde{\alpha} = (1791 \pm \sqrt{332081})/2275$ for the 2 node sets of class 3 on the edges. This leads to a complex value for a coordinate of the latter, so the solution has to be discarded.

The results for $\{M, M', q, v\} = \{6, 9, 13, 1\}$ and $\{6, 9, 13, 2\}$ are new. It is presently unknown if there are other useful solutions for $\{6, 9, 13, 1\}$. For $\{6, 9, 13, 2\}$, the dimension of the null space of the Jacobian is 1. Perturbations of the parameters along that null-space vector converge to slightly different sets of parameters. As mentioned earlier, one could introduce another criterion to further

constrain the choice of node parameters. The table lists a subset of the many elements found, including one with largest (version 2D) and the smallest (version 2E) CFL number discovered so far.

Table 3. Triangular elements of degree M , enriched with polynomials of degree M' in the interior. Numerical quadrature is exact up to and including degree q . Multiple versions are denoted by v. For each of the equivalence classes, the integration weights and parameters that define the node positions, modulo symmetry, are listed. The last column provides a crude estimate of the CFL number.

M	M'	q	v	class	weight	position parameters	CFL
1	1	1		1	1/6		1.14
2	2	2		1	0		
				2	1/6		
2	3	3		1	1/40		0.367
				2	1/15		
				4	9/40		
2	4	4		1	$(11 - \sqrt{13})/720$		0.192
				2	$(5 - \sqrt{13})/45$		
				5	$(29 + 17\sqrt{13})/720$	$(7 - \sqrt{13})/18$	
3	3	4*		1	$-1/120$		
				3	1/20	$\frac{1}{2}(1 - 1/\sqrt{3})$	
				4	9/40		
3	4	5		1	$(8 - \sqrt{7})/720$		0.210
				3	$(7 + 4\sqrt{7})/720$	$1/2 - \sqrt{1/(3\sqrt{7})} - 1/12$	
				5	$7(14 - \sqrt{7})/720$	$(7 - \sqrt{7})/21$	
3	5	6		1	0.00356517965360224101681201		0.122
				3	0.0147847080884026469663777	0.307745941625991646104616	
				5	0.0509423265134759070757019	0.118613686396592868190663	
					0.0825897443227832246413973	0.425340125989747152025431	
4	5	7	1	1	1/315		0.128
				2	4/315		
				3	3/280		
				5	$163/2520 - 47\sqrt{7}/8820$	$\frac{1}{2}(1 - 1/\sqrt{3})$	
					$163/2520 + 47\sqrt{7}/8820$	$(5 - \sqrt{7})/18$	
						$(5 + \sqrt{7})/18$	
4	6	8	1	1	0.00150915593385883937469324		0.0804
				2	0.0101871481261788846308014		
				3	0.00699540146387514358396201	0.199632107119457219140683	
				4	0.0660095591593093891810431		
				5	0.0234436060814549086935898	0.0804959191700374444460458	
				6	0.0477663836054936418696553	0.107591821784867520262175, 0.302912783038363411733216	
5	7	10	1	1	0.000709423970679245979296007		0.0512
				3	0.00348057864048921065844268	0.132264581632713985353888	
					0.00619056500367662911411813	0.363298074153686045705506	
				5	0.0116261354596175711394984	0.0575276844114101056608175	
					0.0459012376307628573770191	0.256859107261959076063891	
					0.0345304303772827935283885	0.457836838079161101938503	
				6	0.0272785759699962595486715	0.0781925836255170219988860, 0.221001218759890007978128	
6	9	12*		1	0.000484273075994968890216176		
				2	0.00324666904899330536180752		
				3	0.00203173085650850495963829	0.100933386433866788849765	
					0.00302271651210398099802707	0.268847661978903971786945	
				4	0.0340548001891207107805596		
				5	0.00804000156250452776502089	0.0484777152222004138468168	
					0.0122972050038284373019703	0.151232747274544209035183	
					0.0177785008242312273394174	0.420707459515049656508480	
				6	0.0171924926132243666716163	0.0497413284921621116798404, 0.369423421302030768191185	
					0.0142325352718470962147968	0.0548913882425097915126526, 0.181151319127438714893044	
					0.0202547332903530326966121	0.168539950027269118385758, 0.284179721960440080344851	

6 9 13 1*	1	0.0000779588662078435375178633		
	2	0.00339681189525519904330250		
	3	0.00065051266109643505640721	0.0279179934866402859608917	
	4	0.00362789876510517486953904	0.241092107358188959592334	
	5	0.0230539870369004268211275	0.208636402173497335322249	
	6	0.00661471763751599238359865	0.0257804392908054300630399,	
		0.0170275218459173680417388	0.0867676995664192358459690	
		0.0169179833927653607471877	0.0472834372836282533842341,	
		0.0193746182487836911462744	0.365554923752573525334004	
			0.0741366666993740353225476,	
			0.183636359341933759692246	
			0.155330109405837631767247,	
			0.489368383573739089292973	
6 9 13 2A	1	0.000457675139493623813925192		0.00349
	2	0.00356710433276790665253250		
	3	0.00200904168539817921681236	0.0983827447888902549102473	
	4	0.00329790979960503607408593	0.265184284071611887908027	
	5	0.00754499275110935015502269	0.0472624300832259203741458,	
	6	0.0204626944006607366113472	0.185099441203658405865967	
		0.000323359777502655800628789	0.223774737049375297733313	
		0.0183536419239484914353561	0.0529938580218328753081271,	
		0.0159637446787891427726817	0.366283836408378472503743	
		0.0223665997042291706303138	0.0599549977665722555070471,	
			0.175353427134619545870900	
			0.169238966075593432510120,	
			0.336402620369427999586902	
6 9 13 2B	1	0.000456928006240664439373013		0.00960
	2	0.00357152911942528341148961		
	3	0.00200874482041614626394457	0.0985365531868998795134592	
	4	0.00329284439557021916630437	0.265248606010655578726896	
	5	0.00752697858686357326415971	0.0471674454162278496208427	
	6	0.0205974639339399517320604	0.18519071803057720879312	
		0.000457338442846254095675932	0.470101135213530921357358	
		0.0181730799890969293541900	0.0529447728826024902425443,	
		0.0159364496926559939859256	0.365369388940646877380306	
		0.0224602643720407294528058	0.0599391280670389459566876,	
			0.175125077083853428192915	
			0.169469754802458550713639,	
			0.494548713123800897107354	
6 9 13 2C	1	0.000457526099467763597178878		0.00544
	2	0.00356872443475518029031584		
	3	0.00200869874130545983070574	0.0983877400941390268764049	
	4	0.00329594726422656522354939	0.265124184082575332680128	
	5	0.00751495983617776527126970	0.0472495946873712019571668	
	6	0.0206027550763567864758638	0.185255094929089930498555	
		0.000146427004224410481372409	0.453454684662496332114277	
		0.0183221247011154001634653	0.0529466980978983572077756,	
		0.0159620953600417771560464	0.366160858287851590299815	
		0.0224286138062640545640809	0.0599621505359141641988445,	
			0.175314126596774109693725	
			0.335975878031815849175464,	
			0.494517960919347201225182	
6 9 13 2D	1	0.000454987233833027795019629		0.0387
	2	0.00355887313687377058494543		
	3	0.00197187750035259785092208	0.0971182187637092591147781	
	4	0.00326405309041122550397833	0.265081457109796002621167	
	5	0.0312076201071798865578207	0.0472995857353385920258670	
	6	0.00751308598168073829542106	0.170113123718258152434644	
		0.0141271046812814012527394	0.416718033745028399150151	
		0.0180228944641299796145248	0.0527759379996054919028731,	
		0.0183416350514485381364864	0.366011227036634594000994	
		0.0152607589589274236884861	0.0580443861948438701313498,	
		0.0174552659654307749558317	0.174910053392499448673606	
			0.171896598740400978122421,	
			0.290177530266989875101690	
6 9 13 2E	1	0.000457122273368821290007004		0.000565
	2	0.00354339780534438440899894		
	3	0.00200624543058909472095270	0.0981884861513482009941253	
	4	0.00328698266411052346335793	0.264562468647341222877659	
	5	0.00296115457958097083809892	0.0472721194967663136860980	
	6	0.00754001264105686566146204	0.185820264979329876077102	
		0.0208058065966998993976974	0.313544917553124746468761	
		0.0105995701595519862981659	0.0524733019403075814209560,	
		0.0181733670633909800708399	0.366393001460113316085618	
		0.0159903777850494079841022	0.0600405892192976491877166,	
		0.0219098798889188534262319	0.175317151926903471833022	
			0.166786803094847451227818,	
			0.495962307385280093776557	

7	10	14*	1	0.000227080483407594748688130	
			3	0.00119069188779806730691585	0.0797278918581723496164217
				0.00209094477794537218122694	0.201362903928456465285586
				0.00267096488057280473904062	0.378955157738687405782957
			5	0.00414456305244987205340665	0.0331662350717603295320680
				0.0215081779064106637197692	0.167165353362395514002772
				0.0236326025323162061101240	0.280558896296460379414635
				0.0142371781018152407429378	0.479984608210471941403749
			6	0.0139626184559205712061905	0.0493368139566529892962173,
				0.0103757635344828902436735	0.280983446243334765057159
				0.0211675487584138389688230	0.0499184036996153092839381,
					0.132175663629467193642302
					0.140658191881288355128006,
					0.342869978275311298138353

The polynomials in the interior are linear combinations of the product of the bubble function $b = xy(1 - x - y)$ and the polynomials in $P_{M'-3} = P_6$. However, the 28 points that should support the Lagrange interpolating polynomials of degree 6 are degenerate for the case $\{6, 9, 13, 1\}$, making this choice unsuitable for finite-element applications.

The elements $\{6, 9, 12\}$ and $\{7, 10, 14\}$ of [6] have too low a value of q in the present context of wave equation modelling. For $\{6, 9, 12\}$, the null space of the Jacobian used in Newton's method has dimension 3 and there exist other nearby solutions. The listed values describe just one of those. For $\{7, 10, 14\}$, there are not enough points to support polynomials in the span of $P_M \oplus P_{M'-3} \times [b]$, with $M = M' = 7$. Instead, a symmetric set can be chosen in the span of $P_7 \oplus P_9 \times [b] \oplus P_1 \times [b^3]$.

Figure 1 shows the distributions of nodes for the simplest elements of degree 1 to 6. Those of degree 6 and with 46 nodes are new. The Jacobian of its corresponding polynomial system has a one-dimensional null space at the root and there are other solutions close to the one

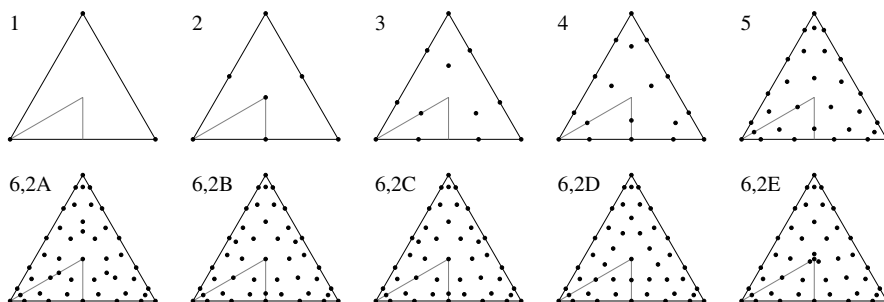


Figure 1. Nodes for the elements of degree M from 1 to 6, mapped to the equilateral triangle. The number of nodes is 3, 7, 12, 18, 30, and 46, for increasing degree. For degree 6, the variants 2A to 2E are shown, from left to right.

shown. The figure displays 5 of the many variants. Among those found so far, variant 6,2D has the largest and 6,2E the smallest CFL number.

4. PERFORMANCE

4.1. Time-stepping Stability

Elements of high degree are more costly than those of lower degree since the number of nodes increases with the degree of the element. The time-stepping stability limit becomes more restrictive at the same time. Elements of higher degree can only be more efficient than those of lower degree if their increased cost can be compensated by using less elements of larger size. The efficiency of an element can be quantified by the computational time needed to obtain a solution with a given accuracy. This will depend on many factors, for instance, code implementation, compilers, hardware, and the chosen problem.

To assess the cost, an estimate of the bound for time-stepping stability is needed. Then, numerical experiments for the constant-density acoustic wave equation are carried out for a simple test problem to determine the efficiency of the various elements.

The standard second-order time discretization of the wave equation is stable if the time step Δt obeys the CFL condition [14], which in this case reads $\Delta t \leq 2/\sqrt{\rho(\mathcal{L})}$, where $\rho(\mathcal{L})$ is the spectral radius of $\mathcal{L} = \mathcal{M}_L^{-1}\mathcal{K}$, the inverse lumped mass matrix \mathcal{M}_L applied to the stiffness matrix \mathcal{K} . One way to estimate this bound is to use the fact that the largest eigenvalue is bounded by the largest row sum of absolute values of \mathcal{L} . Sharper estimates can be found by considering simpler examples, for instance, by Fourier analysis on a periodic mesh. Here, we let $\Delta t \leq \text{CFL} \min(d_i/c)$, where CFL is a constant and $\min(d_i/c)$ denotes the minimum over all elements in the computational domain of the ratio of the diameter, d_i , of the inscribed circle and the the local sound speed, c , for each triangle, taking the largest value over the nodes of that triangle. The constant, CFL, is estimated by considering the spectral radius σ_0 of \mathcal{L}_0 for a unit sound speed on a single reference element with natural (Neumann) boundary conditions. Then, $\text{CFL} = 2/(d_{i,0}\sqrt{\sigma_0})$, where $d_{i,0} = 2 - \sqrt{2}$ is the diameter of the inscribed circle of the reference element. Estimates of CFL obtained in this way are listed in the last column of Table 3. For degrees 1 to 5, [16] estimated values of 1.00, 0.33, 0.23, 0.14 and 0.056, respectively, which agree surprisingly well with the crude estimates 1.14, 0.367, 0.210, 0.128 and 0.0512 found here.

Higher-order time stepping can be accomplished by substituting higher time-derivatives with spatial derivatives using the partial

Table 4. The factor $\sqrt{\sigma_t}$ by which CFL should be multiplied for time stepping of order M_t .

M_t	2	4	6	8	10	12	14	16	18
$\sqrt{\sigma_t}$	1	1.732	1.376	2.317	1.544	2.771	1.569	3.044	1.571

differential equation. This approach is known as the Cauchy-Kovalewski or Lax-Wendroff procedure [17] or the modified equation approach [18] or Dablain’s scheme [19]. For an even time-stepping order M_t , the truncated Taylor series in the absence of source terms is

$$\mathbf{u}^{n+1} - 2\mathbf{u}^n + \mathbf{u}^{n-1} = 2 \sum_{m=1}^{M_t/2} \frac{(\Delta t)^{2m}}{(2m)!} \frac{\partial^{2m} \mathbf{u}^n}{\partial t^{2m}} = 2 \sum_{m=1}^{M_t/2} \frac{(-\Delta t^2 \mathcal{L})^m}{(2m)!} \mathbf{u}^n. \quad (5)$$

Here, \mathbf{u}^n denotes the discrete solution at time $t^n = t^0 + n\Delta t$. The right-hand side involves repeated application of the spatial operator \mathcal{L} . Below, the order of the time-stepping scheme M_t is taken as the smallest even integer larger than or equal to $M + 1$, $M_t = 2 \text{ floor}(1 + \frac{1}{2}M_t)$, with M the degree of the spatial discretization on the edges. The corresponding CFL should then be multiplied by a factor $\sqrt{\sigma_t}$, which can be found by considering the domain of η that corresponds to the range $\beta \in [0, 1]$, where

$$\beta = -\frac{1}{2} \sum_{m=1}^{M_t/2} \frac{(-4\eta)^m}{(2m)!}. \quad (6)$$

Here, η can be identified with any of the eigenvalues of $\frac{1}{4}\Delta t^2 \mathcal{L}$. Expression (6) represents the truncated series of $\sin^2(\sqrt{\eta})$ around $\eta = 0$. If the domain of η is a single interval, σ_t can be taken as its maximum. For $M_t = 10$, two intervals are obtained, $0 \leq \eta \leq 1.54354$ and $1.6052 \leq \eta \leq 2.81526$. In that case, σ_t should be set to the maximum of the leftmost interval, 1.54354. The same approach should be taken for $M_t \geq 14$. Table 4 lists the results for a range of time-stepping orders. The alternating values of $\sqrt{\sigma_t}$ approach $\pi/2$ or π for large M_t .

For $M_t \geq 8$, these results differ from the values in Table 1 of [20], in the row for 1D, multiplied by $2/\pi$ because there, a pseudo-spectral method is considered. [20] has 1.38307 for $M_t = 8$, whereas [21] has 2.317, the same value as found here. For $M_t = 10$, they have 1.38243 and 2.783, respectively, both different from the results listed above. [22] find the same results as reported here. The values in the column labeled with $k = 0$ of their Table 1 are equal to $4\sigma_t$.

4.2. Numerical Experiment

The domain for the test problem is the unit square with a unit propagation speed. A delta-function source at the center emits a waveform $w(t) = [4t/T(1 - t/T)]^8$ for $0 \leq t \leq T$ with a duration $T = 0.1$. The solution on the finite-element nodes at time $t = 1.25$ is compared to the exact solution, shown in Figure 2. Zero Neumann boundary conditions were imposed, reflecting the circular wavefront back into the domain.

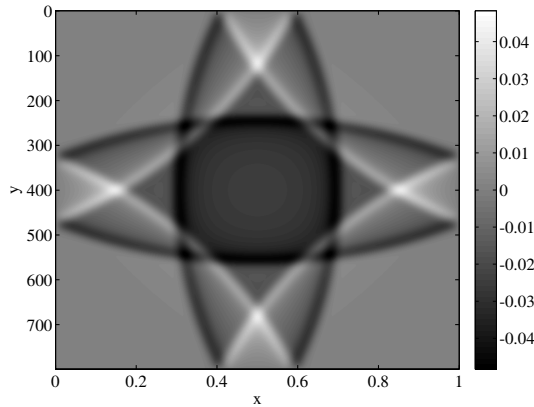


Figure 2. Exact solution for a point source in the center of the unit square with unit speed at time 1.25. The circular wavefront with a positive amplitude has propagated from the source to the boundary, where it was reflected, and back into the domain, passing the center. The boundaries have a reflection coefficient -1 , resulting in a negative amplitude (dark grey). The second reflection is again positive (light grey).

Elements of polynomial degrees $M = 1$ to 6 are considered. For the last, variant 2D is selected since this has the largest CFL number of the elements found so far. For the time step, half of the estimated maximum value is taken to be on the safe side.

As a measure of the accuracy, the maximum error measured at a dimensionless time of 1.25 over all the nodes on the finite-element mesh, divided by the maximum absolute value of the solution, is taken. Figure 3(a) shows this error as a function of $N^{1/2}$, where N is the total number of degrees of freedom. The theoretical asymptotic error curves behave as $N^{-(M+1)/2}$ and are drawn as well. The picture shows that asymptotically, the elements of higher degree are more accurate than those of lower degree. However, what counts in practice is the

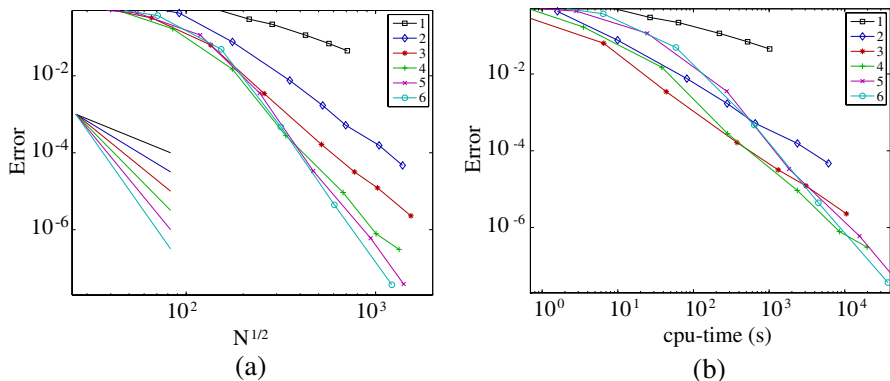


Figure 3. (a) Normalized maximum error over the nodes in the computational domain as a function of $N^{1/2}$, with N the number of nodes or degrees of freedom, for elements of degree 1 to 6. Asymptotically, the higher the order, the smaller is the error. (b) The same errors as a function of the computational time. Elements of degree 3 or 4 are the most efficient, except if very high accuracy is desired.

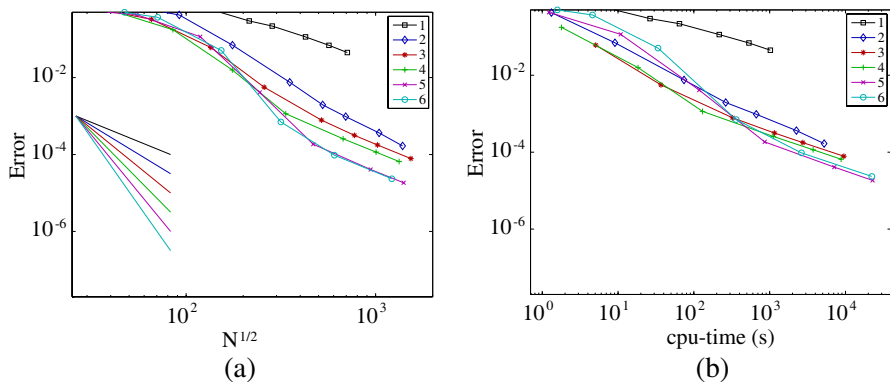


Figure 4. As Figure 3, but with second-order time stepping. At smaller errors, the second-order time-stepping error starts to dominate (a). Again, the elements of degree 3 or 4 are the most efficient (b). For moderate accuracy, the efficiency is nearly the same as with higher-order time stepping.

computational wall-clock time. The behavior of the error as a function of the computational time required for time stepping only is depicted in Figure 3(b). Here, the stiffness matrix was assembled on the fly to save storage, using precomputed matrices for the reference element [4]. For the current test problem, for the lowest degree, $M = 1$, an element of degree 3 or 4 will suffice in practice. Only when very high accuracy is needed, the element of degree 6 will be more efficient.

A time-stepping scheme of second order is less costly than one of higher order. Figure 4 shows results for second-order time stepping and Figure 5 for fourth-order time stepping. Overall, the degree 4 element with fourth-order time stepping is the most efficient.

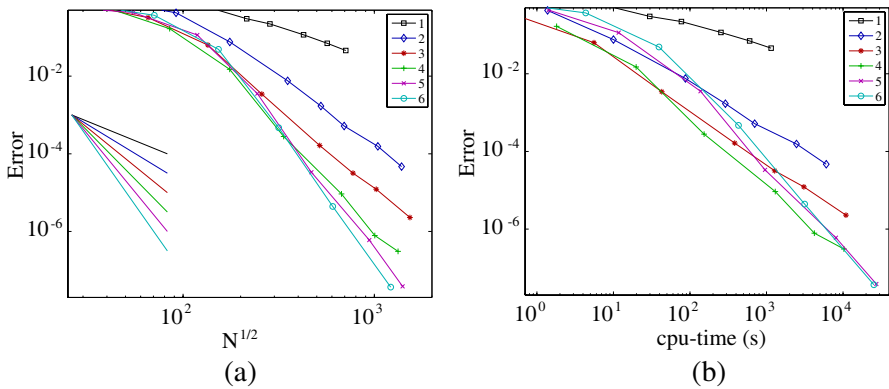


Figure 5. As Figure 3, but with fourth-order time stepping. The degree 4 element is the most efficient.

A comparison between mass-lumped elements up to degree 4 and higher-order finite-difference methods was carried out earlier [4], demonstrating that the finite-difference method is less efficient than the finite-element method in the presence of a sharp contrast in the wave propagation speed.

5. DISCUSSION AND CONCLUSION

Mass-lumped elements of the type described here allow for explicit time stepping and have a spatial accuracy of order $M + 1$ in the element diameter if the degree on the edges is M . Several new elements of degree 6 have been found. Simple estimates of the CFL number that determines the maximum allowable time step show a decrease of this number with increasing degree. The new elements of degree 6 have a wide range of CFL numbers. A comparison of efficiency of elements of

various degrees show that elements of higher degree are more accurate than those of lower degree for a given number of degrees of freedom. In terms of computational time required to reach a given accuracy, however, elements of degree 4 with fourth-order time stepping perform best in a simple example with a known exact solution. The element of degree 6 will only be more efficient if very high accuracy is needed.

It should be noted that there are several alternatives for these types of elements. If one abandons the symmetric arrangement of nodes, quadrature rules based on mapping the square to the reference triangle can be simply obtained from tensorial product orthogonal polynomials [23–27]. [28] considers both asymmetric and symmetric quadrature rules. For the last ones, the known elements of degree 3 and 4 are recovered. Fekete points [29–32] and similar sets of quadrature nodes [33] lead to less accurate quadrature results that still may be useful. Rational functions [34] or sines and cosines [35] can also be considered as basis functions. Discontinuous Galerkin methods [36–38] allow for the use of standard high-order elements. Since the mass matrix is local, it is readily inverted. The price paid is the additional cost of fluxes across the element boundaries. If many source terms need to be considered for the same velocity model, a situation that is common in seismic exploration, a direct sparse-matrix solver for standard higher-order triangular elements will generally be more efficient. The cost of forming the sparse-matrix decomposition is then offset by its inexpensive reuse for multiple source terms.

Applications with mass-lumped finite elements can be found in, for instance, [4, 5, 13, 15, 16, 39].

REFERENCES

1. Fried, I. and D. S. Malkus, “Finite element mass matrix lumping by numerical integration with no convergence rate loss,” *International Journal of Solids and Structures*, Vol. 11, No. 4, 461–466, 1975.
2. Tordjman, N., “Éléments finis d’ordre élevé avec condensation de masse pour l’équation des ondes,” Ph.D. Thesis, L’Université Paris IX Dauphine, 1995.
3. Cohen, G., P. Joly, and N. Tordjman, “Higher order triangular finite elements with mass lumping for the wave equation,” *Proceedings of the Third International Conference on Mathematical and Numerical Aspects of Wave Propagation*, G. Cohen, E. Bécache, P. Joly, and J. E. Roberts, Eds., 270–279, SIAM, Philadelphia, 1995.

4. Mulder, W. A., "A comparison between higher-order finite elements and finite differences for solving the wave equation," *Proceedings of the Second ECCOMAS Conference on Numerical Methods in Engineering*, J.-A. Désidéri, E. Oñate P. Le Tallec, J. Périaux, and E. Stein (eds.), 344–350, John Wiley & Sons, Chichester, 1996.
5. Chin-Joe-Kong, M. J. S., W. A. Mulder, and M. van Veldhuizen, "Higher-order triangular and tetrahedral finite elements with mass lumping for solving the wave equation," *Journal of Engineering Mathematics*, Vol. 35, No. 4, 405–426, 1999.
6. Giraldo, F. X. and M. A. Taylor, "A diagonal-mass-matrix triangular-spectral-element method based on cubature points," *Journal of Engineering Mathematics*, Vol. 56, No. 3, 307–322, 2006.
7. Lyness, J. N. and D. Jespersen, "Moderate degree symmetric quadrature rules for the triangle," *Journal of the Institute of Mathematics and Its Applications*, Vol. 15, 19–32, 1975.
8. Keast, P., "Cubature formulas for the surface of the sphere," *Journal of Computational and Applied Mathematics*, Vol. 17, Nos. 1–2, 151–172, 1987.
9. Heo, S. and Y. Xu, "Constructing fully symmetric cubature formulae for the sphere," *Mathematics of Computation*, Vol. 70, No. 233, 269–279, 2001.
10. Keast, P. and J. C. Diaz, "Fully symmetric integration formulas for the surface of the sphere in s dimensions," *SIAM Journal on Numerical Analysis*, Vol. 20, No. 2, 406–419, 1983.
11. Keast, P., "Moderate-degree tetrahedral quadrature formulas," *Computer Methods in Applied Mechanics and Engineering*, Vol. 55, No. 3, 339–348, 1986.
12. Cohen, G., P. Joly, J. E. Roberts, and N. Tordjman, "Higher order triangular finite elements with mass lumping for the wave equation," *SIAM Journal on Numerical Analysis*, Vol. 38, No. 6, 2047–2078, 2001.
13. Mulder, W. A., "Higher-order mass-lumped finite elements for the wave equation," *Journal of Computational Acoustics*, Vol. 9, No. 2, 671–680, 2001.
14. Courant, R., K. Friedrichs, and H. Lewy, "Über die partiellen Differenzgleichungen der mathematischen Physik," *Mathematische Annalen*, Vol. 100, No. 1, 32–74, 1928.
15. Zhebel, E., S. Minisini, A. Kononov, and W. A. Mulder, "Solving the 3D acoustic wave equation with higher-order mass-lumped

- tetrahedral finite elements,” *73rd EAGE Conference & Exhibition, Extended Abstracts*, A010, Vienna, Austria, May 2011.
16. Jund, S. and S. Salmon, “Arbitrary high-order finite element schemes and high-order mass lumping,” *International Journal of Applied Mathematics and Computer Science*, Vol. 17, No. 3, 375–393, 2007.
 17. Lax, P. and B. Wendroff, “Systems of conservation laws,” *Communications on Pure and Applied Mathematics*, Vol. 31, No. 2, 217–237, 1960.
 18. Shubin, G. R. and J. B. Bell, “A modified equation approach to constructing fourth order methods for acoustic wave propagation,” *SIAM Journal on Scientific and Statistical Computing*, Vol. 8, No. 2, 135–151, 1987.
 19. Dablain, M. A., “The application of high-order differencing to the scalar wave equation,” *Geophysics*, Vol. 51, No. 1, 54–66, 1986.
 20. Chen, J.-B., “Lax-Wendroff and Nyström methods for seismic modelling,” *Geophysical Prospecting*, Vol. 57, No. 6, 931–941, 2009.
 21. De Basabe, J. D. and M. K. Sen, “Stability of the high-order finite elements for acoustic or elastic wave propagation with high-order time stepping,” *Geophysical Journal International*, Vol. 181, No. 1, 577–590, 2010.
 22. Gilbert, J. C. and P. Joly, “Higher order time stepping for second order hyperbolic problems and optimal CFL conditions,” *Computational Methods in Applied Sciences*, Vol. 16, 67–93, Springer, Berlin, 2008.
 23. Koornwinder, T., “Two-variable analogues of the classical orthogonal polynomials,” *Theory and Application of Special Functions*, R. A. Askey (ed.), 435–495, Academic Press, New York, 1975.
 24. Dubiner, M., “Spectral methods on triangles and other domains,” *Journal of Scientific Computing*, Vol. 6, No. 4, 345–390, 1991.
 25. Sherwin, S. J. and G. E. Karniadakis, “A new triangular and tetrahedral basis for high-order (hp) finite element methods,” *International Journal for Numerical Methods in Engineering*, Vol. 38, No. 22, 3775–3802, 1995.
 26. Heinrichs, W. and B. I. Loch, “Spectral schemes on triangular elements,” *Journal of Computational Physics*, Vol. 173, No. 1, 279–301, 2001.
 27. Bittencourt, M. L., “Fully tensorial nodal and modal shape functions for triangles and tetrahedra,” *International Journal for*

- Numerical Methods in Engineering*, Vol. 63, No. 11, 1530–1558, 2005.
28. Xu, Y., “On Gauss-Lobatto integration on the triangle,” *SIAM Journal on Numerical Analysis*, Vol. 49, No. 2, 541–548, 2011.
 29. Taylor, M. A., B. A. Wingate, and R. E. Vincent, “An algorithm for computing Fekete points in the triangle,” *SIAM Journal on Numerical Analysis*, Vol. 38, No. 5, 1707–1720, 2000.
 30. Bos, L., M. A. Taylor, and B. A. Wingate, “Tensor product Gauss-Lobatto points are Fekete points for the cube,” *Mathematics of Computation*, Vol. 70, No. 236, 1543–1547, 2001.
 31. Pasquetti, R. and F. Rapetti, “Spectral element methods on triangles and quadrilaterals: Comparisons and applications,” *Journal of Computational Physics*, Vol. 198, No. 1, 349–362, 2004.
 32. Wingate, B. A. and M. A. Taylor, “Performance of numerically computed quadrature points,” *Applied Numerical Mathematics*, Vol. 58, No. 7, 1030–1041, 2008.
 33. Hesthaven, J. S., “From electrostatics to almost optimal nodal sets for polynomial interpolation in a simplex,” *SIAM Journal on Numerical Analysis*, Vol. 35, No. 2, 655–676, 1998.
 34. Shen, J., L.-L. Wang, and H. Li, “A triangular spectral element method using fully tensorial rational basis functions,” *SIAM Journal on Numerical Analysis*, Vol. 47, No. 3, 1619–1650, 2009.
 35. Li, H., J. Sun, and Y. Xu, “Discrete Fourier analysis, cubature and interpolation on a hexagon and a triangle,” *SIAM Journal on Numerical Analysis*, Vol. 46, No. 4, 1653–1681, 2008.
 36. Rivière, B. and M. F. Wheeler, “Discontinuous finite element methods for acoustic and elastic wave problems,” *Contemporary Mathematics*, Vol. 329, 271–282, 1999.
 37. De Basabe, J. D., M. K. Sen, and M. F. Wheeler, “The interior penalty discontinuous Galerkin method for elastic wave propagation: Grid dispersion,” *Geophysical Journal International*, Vol. 175, No. 1, 83–93, 2008.
 38. Käser, M. and M. Dumbser, “An arbitrary high-order Discontinuous Galerkin method for elastic waves on unstructured meshes — I. The two-dimensional isotropic case with external source terms,” *Geophysical Journal International*, Vol. 166, No. 2, 855–877, 2006.
 39. Lesage, A. C., R. Aubry, G. Houzeaux, M. Araya Polo, and J. M. Cela, “3D spectral element method combined with H-refinement,” *72nd EAGE Conference & Exhibition*, Extended Abstracts, C047, Barcelona, Spain, Jun. 2010.